

© 2006 by Matthew C. Zwier. All rights reserved.

COMPUTATIONAL AND SPECTROSCOPIC CHALLENGES OF PROTONATED  
METHANE

BY

MATTHEW C. ZWIER

B.S., Hope College, 2003

THESIS

Submitted in partial fulfillment of the requirements  
for the degree of Master of Science in Chemistry  
in the Graduate College of the  
University of Illinois at Urbana-Champaign, 2006

Urbana, Illinois

*To my father, my first and foremost scientific and personal mentor.*

# Acknowledgements

The author extends deep thanks to Anne McCoy (OSU) and Joel Bowman and Xinchuan Huang (Emory University) for providing copies of original data. Diffusion Monte Carlo data from the McCoy group enabled the rotational analysis of Section 3.1, and geometries and MULTIMODE vibrational frequencies from the Bowman group enabled the discussion of Section 3.2.

# Table of Contents

<b>Chapter 1 Introduction</b> . . . . .	1
1.1 $\text{CH}_5^+$ in Euclidean Space . . . . .	1
1.2 Structure and Classical/Quantum Correspondence . . . . .	3
1.3 Energetics, Structure, and Tunneling . . . . .	4
1.4 Foundational Work on $\text{CH}_5^+$ . . . . .	8
1.5 Considerations for Spectral Analysis . . . . .	9
<b>Chapter 2 Theoretical Studies of <math>\text{CH}_5^+</math></b> . . . . .	10
2.1 Zero-Point Vibrational Energy Effects . . . . .	10
2.2 Electronic Structure of $\text{CH}_5^+$ . . . . .	12
2.2.1 Early Electronic Structure Calculations . . . . .	12
2.2.2 Modern Electronic Structure Calculations . . . . .	13
2.3 Classical and Quantum Dynamics of $\text{CH}_5^+$ . . . . .	16
2.3.1 Early Dynamics Efforts . . . . .	17
2.3.2 Recent Dynamics Efforts . . . . .	18
2.4 The Particle-on-a-Sphere Model . . . . .	19
2.5 Symmetry Analysis . . . . .	20
2.5.1 Nuclear Spin Statistics . . . . .	20
2.5.2 Equivalent Rotations of $\text{CH}_5^+$ . . . . .	20
<b>Chapter 3 Predicted Spectral Features of <math>\text{CH}_5^+</math></b> . . . . .	22
3.1 Rotational Features . . . . .	22
3.2 Vibrational Features . . . . .	26
<b>Chapter 4 Summary, Conclusions, and Future Directions</b> . . . . .	31
4.1 Variational Calculations on $\text{CH}_5^+$ . . . . .	32
4.2 Future Prospects . . . . .	34
<b>References</b> . . . . .	35

# Chapter 1

## Introduction

The methonium ion,  $\text{CH}_5^+$ , is a shining example of how a relatively simple system can exhibit incredibly complex behavior. Discovered in 1952 by Tal'roze and Lyubimova,<sup>1</sup>  $\text{CH}_5^+$  is viewed both as prototypical, having the same form as intermediates in organic  $\text{S}_{\text{N}}1$  substitution reactions, and unique, because of its highly anharmonic internal motion and extensive delocalization of nuclei. Furthermore,  $\text{CH}_5^+$  is thought to be the precursor to all carbon chains in the interstellar medium. Seemingly of fundamental importance, the methonium ion has been the subject of extensive theoretical and experimental study. Experimental observation has proven extremely difficult; for example, Oka's group obtained an unassignable spectrum after fifteen years of effort.<sup>2</sup> Much focus has therefore been given to theoretical consideration of the nature of  $\text{CH}_5^+$ .

With only six nuclei and ten electrons, one might initially expect that electronic structure calculations would provide adequate insight into the structure and behavior of this ion. With so few electrons, relatively high-level calculations could be employed with ease. However, the very concept of the geometry of  $\text{CH}_5^+$  becomes problematic, as one considers the seemingly-mutually-exclusive constraints imposed by Euclidean space and the precepts of quantum mechanics.

### 1.1 $\text{CH}_5^+$ in Euclidean Space

There is no way to distribute five points equivalently in three dimensions, and thus the five protons of  $\text{CH}_5^+$  should be chemically inequivalent. In place of a rigorous (and intu-

itively unenlightening) proof of that bald statement, consider the crystallographic point groups. The spherical groups, those with centers distributed equivalently, represent only tetrahedral, octahedral, and icosahedral structures. Such structures can be considered to have four, six, and twelve vertices, respectively, regardless of the number of centers involved. For example,  $C_{60}$ , of  $I_h$  symmetry, has sixty centers; each vertex of the corresponding icosahedron is defined by five carbon atoms. The entire span of remaining crystallographic groups have their centers distributed unequally through Euclidian space. Indeed, electronic structure calculations indicate that possible arrangements for  $\text{CH}_5^+$  include  $C_s$ ,  $C_{2v}$ ,  $D_{3h}$ , and  $C_{4v}$  forms,<sup>3</sup> among others, which are readily seen to have inequivalent placement of protons.

Quantum mechanically, however, the protons in  $\text{CH}_5^+$  are identical fermions, so for any given molecular geometry, there are  $5! = 120$  possible equivalent minima. Depending on the energetic barriers for transitions among these minima, a very different picture of the nature of  $\text{CH}_5^+$  emerges. In the limit of high barriers between minima, the protons are indeed chemically inequivalent, as they are unevenly distributed in space and localized in their respective positions. In the limit of moderate or low barriers, however, the protons should be able to exchange via tunneling. In this tunneling regime, the protons must be equivalent if they are able to access all 120 minima on a given timescale. In the Born-Oppenheimer quasiclassical view of molecular structure, such tunneling action appears as internal rotation, where after projecting out global molecular rotation, the protons still seem to “wander” about. This apparent internal motion has led Müller and others to comment that “the very concept of molecular structure becomes problematic for this molecule.”<sup>4</sup>

## 1.2 Structure and Classical/Quantum Correspondence

One might argue that the difficulty in understanding the “structure” of  $\text{CH}_5^+$  is not only in the nature of the ion, but also in the inherent discrepancy between the classical notion of molecular structure and the quantum-mechanical reality of the physics describing the ion. To say that a molecule has a structure, or a set of structures, inherently reduces the nuclei of the molecule from diffuse, wavelike quantum mechanical objects to classical particles. While such a reduction is intuitive and informative — and perhaps even necessary to our practical understanding of chemistry as a whole — we must immediately re-classify fundamentally quantum effects in semi-classical terms. For example, the quantum mechanical delocalization of nuclei becomes the zero-point vibrational motion. Tunneling becomes internal rotation. To say a molecule has a structure is to assert that the nuclei are well-localized in certain regions of space; therefore any significant delocalization of nuclei leads to an immediate breakdown of the concept of structure.

The analysis of the nature of  $\text{CH}_5^+$  therefore requires clear separation between an intuitive classical world-view and accurate quantum-mechanical interpretation. Each reduction of the quantum nature of  $\text{CH}_5^+$  to a more convenient classical picture should, ideally, be examined and justified.

Such a pattern of justification goes far beyond the philosophical question of “how to think” about the methonium ion. The analysis of spectroscopic results frequently hinges upon reduction of a quantum-mechanical Hamiltonian to separate classical terms which are then transformed into their corresponding quantum operators. The familiar decomposition of the molecular Hamiltonian to electronic, vibrational, and rotational parts is perhaps the best example. But how can one define a rotational Hamiltonian for a system whose moment of inertia is constantly changing as protons rearrange within the molecule? How can one define a vibrational Hamiltonian if there is no single global minimum structure around which to expand a potential?

To have any hope of interpreting a high-resolution spectrum of  $\text{CH}_5^+$ , an accurate model Hamiltonian will be required, and such a Hamiltonian can only be constructed when the quantum mechanics of the ion is sufficiently well-understood. As in any non-trivial system, this will require an iterative approach, with quantum theory explaining experimental results and experimental results directing the refinement of theory.

### 1.3 Energetics, Structure, and Tunneling

The primary challenge to both experimental interpretation and theoretical consideration of  $\text{CH}_5^+$  is the probable absence of a distinct “structure” for the ion. As mentioned above, to say a molecule has a structure is to imply that its nuclei are well-localized. This inherently semiclassical view of molecular structure is intuitive, and couples very well with the Born-Oppenheimer (B-O) approximation. The B-O approximation asserts that given the three-order-of-magnitude difference in mass between electrons and nuclei, the electrons move with respect to essentially fixed nuclei. The positions of the nuclei therefore parametrically determine the potential field which governs electronic motion, and the resulting electronic structure determines the potential field in which the nuclei interact. This leads directly to the familiar concept of the potential energy surface (PES), the hypersurface defined by the electronic potential energy of the system as a function of nuclear coordinates. The nuclei can then be viewed as semiclassical particles interacting on this PES, with the electronic structure instantaneously adapting to (and therefore determining) nuclear motion.

The equilibrium structure of the molecule, therefore, is readily and intuitively defined as the nuclear configuration at which the potential energy is at a minimum. Transition states are saddle points on the PES connecting local minima.<sup>5</sup> The energy of a transition state with respect to that at a local minimum is the familiar transition state barrier height, determining the likelihood of the system crossing that transition state to another mini-

num. The most stable configuration, of course, is the nuclear configuration at which the potential is at a global minimum.

The Born-Oppenheimer approximation thus separates the electronic and nuclear motions and provides theoretical descriptions of structures, transition states, and the energies needed to rearrange the molecule from one structure to another. From these concepts, one can build up the familiar semiclassical pictures of separated motions. Molecular rotation depends on the moments of inertia defined by the lowest-energy nuclear configuration. Molecular vibration occurs about the same configuration.

With this convenient definition of molecular vibration comes an immediate problem: what happens when the nuclei rearrange across a transition state? First, one must make some careful definitions. Consider the prototypical double well, with various barrier heights, as illustrated in Figure 1.1. Since we seek information about the most stable ground-state structure of  $\text{CH}_5^+$ , the only energy available to the system to allow for nuclear rearrangement is zero-point vibrational energy (ZPVE,  $E_{\text{ZP}}$ ).

In classical mechanics, a potential barrier separates two regions of phase space, and the barrier can be surmounted if and only if the kinetic energy of the system exceeds the height of the barrier. In that case, the system has absolute freedom to explore both regions of phase space, as illustrated in the left panel of Fig. 1.1. If the energy of the system does not exceed the barrier height, the system is strictly localized to one region of phase space (Fig. 1.1, right).

In quantum mechanics, a barrier localizes wavefunction density, but tunneling can allow density to “leak” through the barrier, with probability exponentially decreasing with increasing barrier height (relative to the energy of the system). The quantum system behaves much like the classical system in both extremes. When energy is significantly greater than the barrier ( $E_{\text{ZP}} \gg V_{\text{barrier}}$ , Fig. 1.1), then the wavefunction delocalizes freely. When energy is significantly less than the barrier ( $E_{\text{ZP}} \ll V_{\text{barrier}}$ , Fig. 1.1, right), then the wavefunction is strongly localized in one potential region, owing to the exponentially-

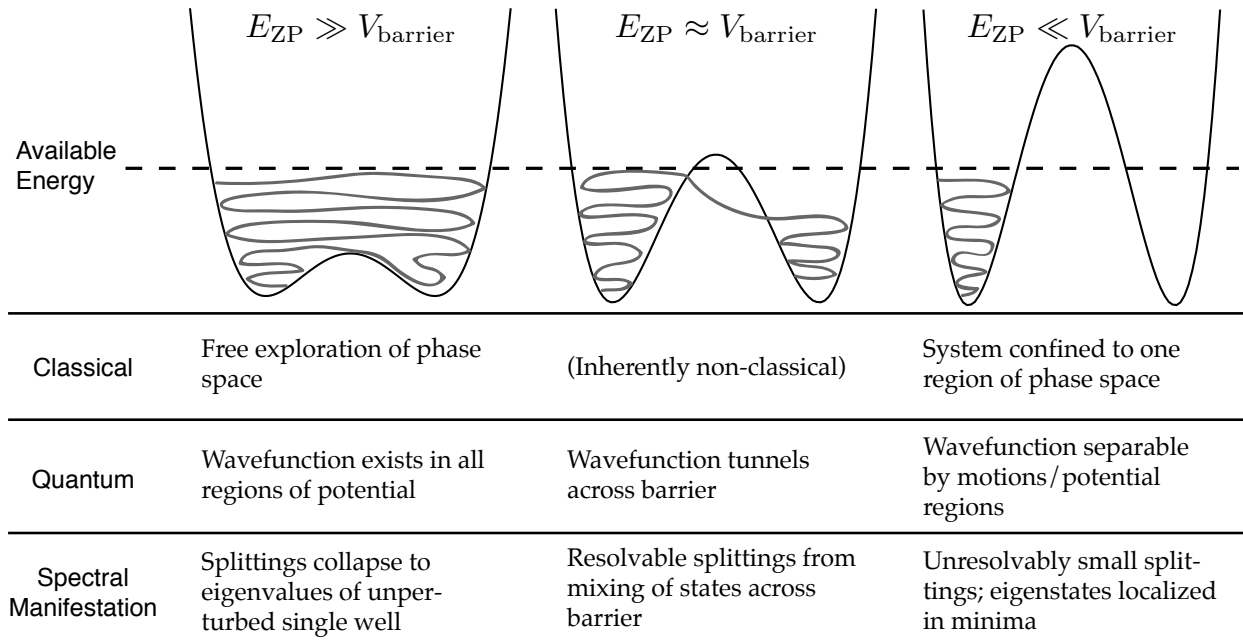


**Figure 1.1: Prototypical double potential well with various barrier heights.**

Given a particle with certain available energy (in a ground-state system, the zero point vibrational energy  $E_{ZP}$ ) the classical and quantum mechanics of the particle in wells of differing barrier heights  $V_{\text{barrier}}$  are noted, as are the spectral features resulting from each case.

decreasing nature of tunneling. In the intermediate case, where available energy is on the order of the barrier height, tunneling allows wavefunction density to disperse across the barrier (Fig. 1.1, center).

Since in the extreme cases  $E_{ZP} \gg V_{\text{barrier}}$  and  $E_{ZP} \ll V_{\text{barrier}}$  the quantum mechanical system and classical mechanical system behave similarly, one would expect semi-classical descriptions of the system to hold. Under that assumption, consider one particle moving in the one-dimensional wells pictured in Fig. 1.1. In the low-barrier case, a classical particle would explore a large region of phase space, and a quantum particle would freely delocalize over a large region of the potential. These pictures are consistent with each other; in both cases, the probability of finding the particle is spread throughout the well; the barrier might as well not exist. A spectrum of such a system would contain a single feature, corresponding to the single region of potential the quantum particle can explore.

In the high-barrier case, a classical particle is confined to a smaller region of phase

space, and a quantum particle is more localized; one may freely consider the two potential regions to be separable. A spectrum would again contain a single feature, but in this case because the particle is equally likely to be in either of two identical wells.

In the intermediate barrier case,  $E_{ZP} \approx V_{\text{barrier}}$ , no classical comparison exists, and the quantum particle can delocalize across the barrier with a concomitant decrease in probability density. Here, spectral splitting would be observed, as the two sides of the well are no longer quantum-mechanically equivalent, at least after the observation. Visualizing loosely, imagine placing a particle in the double well. One does not know in advance whether it will fall to the left or right of the barrier, but once it has, the other side must have lower density as the wavefunction accesses it through tunneling.

Here, the consideration of nuclear motion in semiclassical terms becomes tenuous at best. Properly, one configuration tunneling into another is an indication of quantum delocalization; one does not know which state the system is in until a measurement occurs. The best classical analogy is that the system has rearranged, which implies localization at both beginning and end configurations and *at every point along the way*. This leads to a picture of “internal motion”, where some vibrational mode carries a nuclear configuration across a transition state to a different nuclear configuration. In  $\text{CH}_5^+$ , this process is often called “hydrogen scrambling.” As the underlying principle is nuclear delocalization, no such motion need actually occur in the classical sense. Thus, in constructing a model Hamiltonian for  $\text{CH}_5^+$ , one must evaluate whether it is reasonable to treat a tunneling path as a vibrational mode.

Finally, the effect of the tunneling motion (delocalization) on other semiclassical assumptions must be evaluated. In constructing a vibrational potential expansion or rigid-rotor moments of inertia, which B-O minimum should be selected as the reference state? Should the transition state, in some sense an average of the possible stationary points, be selected instead? Is there any reasonable semiclassical alternative to considering the delocalized (tunneling) nuclei as a probability density distribution? All of these questions

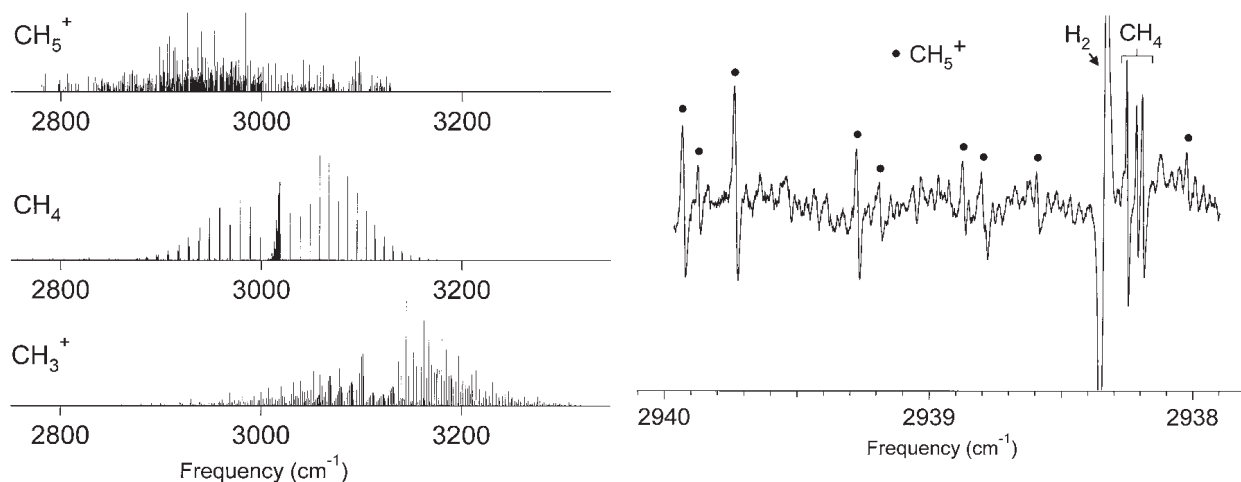


**Figure 1.2: Oka's group's spectrum of  $\text{CH}_5^+$**

Bands due to  $\text{CH}_5^+$  were identified by removing signal from neutrals and from well-known spectra of other carbocations. Signal due to  $\text{CH}_4^+$  may remain.<sup>10</sup>

must be considered in the analysis of the nature (and hence spectra) of  $\text{CH}_5^+$ .

## 1.4 Foundational Work on $\text{CH}_5^+$

Prior to the advent of practical electronic structure methods, the five protons in  $\text{CH}_5^+$  were considered equivalent,<sup>6</sup> which by the above geometrical argument would require delocalization of hydrogen nuclei. As early as 1972, electronic structure calculations on  $\text{CH}_5^+$  showed that the lowest-energy stationary point consisted of a  $\text{H}_2$  unit strongly bound to a  $\text{CH}_3^+$  unit, with nearby low-lying  $C_s$  and  $C_{2v}$  transition states.<sup>7,8</sup> Though continually debated, ever-advancing electronic structure calculations consistently reproduce this result.<sup>3,4,6,9</sup>

Because of the difficulty of obtaining gas-phase  $\text{CH}_5^+$  in the absence of interfering species such as hot  $\text{CH}_4$  and  $\text{CH}_3^+$ , only in the last few years have spectra of  $\text{CH}_5^+$  been recorded. The first spectrum was obtained by Oka's group in 1999,<sup>10</sup> and remained the only spectrum of  $\text{CH}_5^+$  until the Marx group recorded a low resolution action spectrum in 2005.<sup>11</sup> The spectrum recorded by the Oka group was a combination of bands due to

$\text{CH}_5^+$ ,  $\text{CH}_4$ , and  $\text{CH}_3^+$ , and the  $\text{CH}_5^+$  spectrum was derived by weeding out the known signals of  $\text{CH}_4$  and  $\text{CH}_3^+$  (and other carbocations). The high temperature conditions of the positive column apparatus used led to an unassignably-complicated spectrum, shown in Fig. 1.2. As an additional complication, the spectrum of  $\text{CH}_4^+$  is unrecorded; though White *et al.* assert it to be a minor species in hydrogen-dominated  $\text{H}_2 - \text{CH}_4$  plasmas, the authors acknowledge that the existence of spurious lines due to  $\text{CH}_4^+$  cannot be completely discounted.<sup>10</sup>

## 1.5 Considerations for Spectral Analysis

Obtaining and analyzing a low-temperature, high-resolution spectrum of  $\text{CH}_5^+$  will undoubtedly be a considerable task, but one which will be mitigated by careful theoretical analysis. First, a vibrational band must be selected for study. Because of the highly anharmonic and delocalized nature of  $\text{CH}_5^+$ , this in itself is a non-trivial issue. Having selected a vibrational band, the rotational structure of the band must be investigated; this also will be a significant task, as tunneling motions will likely split the observed rotational levels. Taken together, these issues point to the larger issue of what internal motions will define the overall rovibrational levels of the system. In the case of free hydrogen exchange (tunneling), it has been theorized that the only good quantum numbers for  $\text{CH}_5^+$  are the total angular momentum, parity, and nuclear spin angular momentum,<sup>10</sup> so the construction of a Hamiltonian for fitting rovibrational levels may not necessarily correspond to intuitive notions of vibration and rotations. A key question to be investigated in advance of obtaining a spectrum, then, is how reliably one can use semiclassical arguments to understand  $\text{CH}_5^+$ .

# Chapter 2

## Theoretical Studies of $\text{CH}_5^+$

The umbrella term “theory” can imply anything from a scratch pad to a supercomputer, and both types of theory have seen extensive application toward  $\text{CH}_5^+$ . Computational theory has generally been more fruitful, as it sidesteps most of the questions about how to think about the ion, imposing its own well-understood limitations. Most branches of computational chemistry have at least touched  $\text{CH}_5^+$  at some point.

Stationary point calculations have seen the most use, especially in the development of Born-Oppenheimer potential energy surfaces used in further study of  $\text{CH}_5^+$ . Classical molecular dynamics simulations on such surfaces have been used to visualize the internal dynamics of hydrogen scrambling. Quantum dynamics calculations have been used to construct a ground-state wavefunction with an accuracy midway between stationary point calculations and variational calculations. Such variational calculations are currently the standard for connecting computational theory and high-resolution spectroscopy, yielding highly-accurate energy levels directly; such calculations have not yet been employed on a system as large as  $\text{CH}_5^+$ . All of these methods and their results for  $\text{CH}_5^+$  will be discussed below.

### 2.1 Zero-Point Vibrational Energy Effects

Before embarking on an exegesis of the electronic structure of  $\text{CH}_5^+$ , the concept of zero-point vibrational energy must be discussed in the context of the Born-Oppenheimer approximation. A chemical species at a B-O stationary point *must* contain energy due to

vibrational motion. Equivalently, the Uncertainty Principle dictates that nuclei must be delocalized, at least to some extent. Therefore, the relative energies of states depend on the zero-point energy  $E_{ZP}$ . For a given nuclear configuration  $\vec{Q}$ , the overall energy  $E_0$  of the system is

$$E_0(\vec{Q}) = E_e(\vec{Q}) + E_{ZP}(\vec{Q}) \quad (2.1)$$

where  $E_e$  is the Born-Oppenheimer electronic energy and  $E_{ZP}$  is the zero-point vibrational energy (expanded about  $\vec{Q}$ ). Thus, the difference in energy  $\Delta E_0$  between two states at structures  $\vec{Q}_1$  and  $\vec{Q}_2$  is

$$\Delta E_0(\vec{Q}_1, \vec{Q}_2) = \Delta E_e(\vec{Q}_1, \vec{Q}_2) + \Delta E_{ZP}(\vec{Q}_1, \vec{Q}_2) \quad (2.2)$$

Thus, the correct ordering of states requires inclusion of zero-point energy effects. In terms of nuclear delocalization, greater tendency to delocalize (larger  $E_{ZP}$ ) about some geometry  $\vec{Q}$  may stabilize or destabilize that configuration with respect to others.

Since ZPVE is a semiclassical concept, it of course somewhat ill-defined. The total zero-point energy of a potential minimum is simply the sum of the zero-point energies of all the normal modes:

$$E_{ZP} = \sum_{k=1}^{3N-6} E_{ZP(k)} \quad (2.3)$$

However, at a first-order saddle point on the PES (*i.e.* a transition state), the vibrational frequency corresponding to the mode across the transition state is imaginary and does not contribute to the ZPVE of the system:

$$E_{ZP} = \sum_{k=1}^{3N-7} E_{ZP(k)} \quad (2.4)$$

This is intuitive in a semiclassical world-view, as momentum from all other normal modes contributes to the total energy of the system (in the usual  $E = (\vec{p})^2/2m$  sense), but momentum along the barrier-crossing coordinate is *used* for surmounting the barrier, and

therefore cannot contribute additively to the total energy of the system.

## 2.2 Electronic Structure of $\text{CH}_5^+$

Until very recently, most of the computational study of  $\text{CH}_5^+$  has necessarily been limited to Born-Oppenheimer molecular orbital calculations. Non-Born-Oppenheimer calculations have only recently emerged and are developing in parallel with computing technology; they have not been applied to systems larger than diatomics.<sup>12</sup> While ultimately the reliability of treating the ion in this way will be decided by spectroscopic results, even low-level B-O calculations have offered much insight into the nature of  $\text{CH}_5^+$ .

### 2.2.1 Early Electronic Structure Calculations

Very shortly after the advent of computational electronic structure theory, theorists turned their attention to the disputed question of the structure of  $\text{CH}_5^+$ . The earliest studies assumed a maximally-symmetric  $D_{3h}$  structure and employed empirical or very limited molecular orbital calculations,<sup>13</sup> but soon the development of the semiempirical CNDO (complete neglect of differential overlap) method allowed more precise and generic energy calculations. In early 1969, Gamba *et al.* published results in which a  $C_S$  structure, reminiscent of  $\text{H}_2$  and  $\text{CH}_3^+$  subunits, was calculated to be approximately 10 kcal/mol more stable than the symmetric  $D_{3h}$  structure<sup>14</sup>.

This spurred a slew of studies on  $\text{CH}_5^+$ , with often-conflicting results.<sup>13</sup> Dyczmons *et al.* performed Hartree-Fock calculations on  $\text{CH}_5^+$  in optimized  $D_{3h}$ ,  $C_{4v}$ ,  $D_{2h}$ , and two independent  $C_S$  configurations. Employing fully *ab initio* Hartree-Fock calculations over a minimal but optimized basis set, the authors confirmed a  $C_S$  structure to be the lowest-energy configuration. The two  $C_S$  structures were nearly identical in energy, indicating nearly free rotation of the  $\text{H}_2$  moiety with respect to the  $\text{CH}_3^+$  unit. There was evidence of three-center two-electron bonding between the  $\text{H}_2$  unit and the central carbon. Confident

in their calculations, the authors boldly state, "The question of the equilibrium geometry of the  $\text{CH}_5^+$ -ion can be regarded as settled."<sup>13</sup>

Shortly thereafter, the Pople group turned their efforts towards characterizing entire series of hydrocarbon cations. Using Hartree-Fock calculations over larger split-valence basis sets, the authors confirmed a  $C_S$  minimum-energy structure.<sup>7</sup> Employing larger basis sets including polarization functions further stabilizes the  $C_S$  structure.<sup>15</sup>

The first evidence of complete proton scrambling came in 1974 with further work by Dyczmons and Kutzelnigg. With a basis set similar to that used in Ref. 15, the authors confirm that the  $C_S$  structure is of minimum energy, but with the inclusion of electron correlation effects, a nearby  $C_{2v}$  stationary point becomes nearly identical in energy within the estimated uncertainty of  $\sim 5$  kcal/mol. As the  $C_{2v}$  structure is a transition state between equivalent  $C_S$  minima and the  $\text{H}_2$  unit seems capable of free rotation, the authors conclude that "at room temperature, all the protons are dynamically equivalent."<sup>8</sup>

With the advent of ion cyclotron resonance data on  $\text{CH}_5^+$  in 1974, the  $C_S$  structure was seemingly confirmed, with some indication that the hydrogens are chemically inequivalent. From this it was concluded that  $\text{CH}_5^+$  does not readily undergo proton scrambling,<sup>16</sup> in contradiction of Dyczmons and Kutzelnigg.

## 2.2.2 Modern Electronic Structure Calculations

After the development of computers sufficiently powerful to employ Møller-Plesset perturbation theory over relatively large basis sets, focus quickly returned to  $\text{CH}_5^+$ . In the impressively-numbered fortieth paper in Pople's series on the electronic structure of organic molecules, Raghavachari *et al.* revisit the structure of  $\text{CH}_5^+$  using second- (MP2), third- (MP3), and partial fourth-order [MP4(SDQ)] perturbation theory to introduce electron correlation effects into the Hartree-Fock wavefunction. With the contemporaneous availability of analytic second derivatives of energy with respect to nuclear displacement,

it became possible to characterize the natures of the various stationary points of  $\text{CH}_5^+$ . The authors found that only the lowest-energy  $C_S$  structure was a minimum, and that the nearby higher-energy  $C_S$  and  $C_{2v}$  structures were transition states. The extremely small energy difference (0.1 kcal/mol) between the minimum [typically labeled  $C_s(\text{I})$ ] and the lowest-lying transition state [ $C_s(\text{II})$ ] support the notion that  $\text{CH}_5^+$  exhibits essentially unhindered rotation of the  $\text{H}_2$  group with respect to the  $\text{CH}_3^+$  group. The  $C_{2v}$  transition state is only higher in energy by 0.6 – 1.1 kcal/mol at various orders of perturbation. This would allow hindered exchange of hydrogen nuclei between the  $\text{CH}_3^+$  and  $\text{H}_2$  groups, indicating that the five protons may undergo complete scrambling.<sup>17</sup> These structures and interconversion pathways and are shown in Figure 2.1, a particularly clear rendition due to Schreiner.<sup>6</sup>

As computing power increased, analysis turned to continually more powerful post-SCF methods. Analysis treating electron correlation with configuration interaction methods confirmed the Pople group's 1981 results.<sup>18</sup> More support for the possibility of hydrogen rearrangement was presented by von Ragué Schleyer, who first concluded that when zero-point vibrational energy corrections were considered, all of the  $C_s(\text{I})$ ,  $C_s(\text{II})$ , and  $C_{2v}$  structures are essentially identical in energy, and therefore  $\text{CH}_5^+$  should exhibit complete proton scrambling even as the temperature approaches 0 K.<sup>19</sup> Even very recent stationary point calculations indicate that the  $C_s(\text{II})$  state is  $10.6 \text{ cm}^{-1}$  and the  $C_{2v}$  state  $150.6 \text{ cm}^{-1}$  more stable than the  $C_s(\text{I})$  state when ZPVE corrections are applied.<sup>9</sup>

These results are summarized in Table 2.1. Clearly, fundamentally quantum effects, particularly nuclear delocalization, play a key role in the structure/internal dynamics of  $\text{CH}_5^+$ .

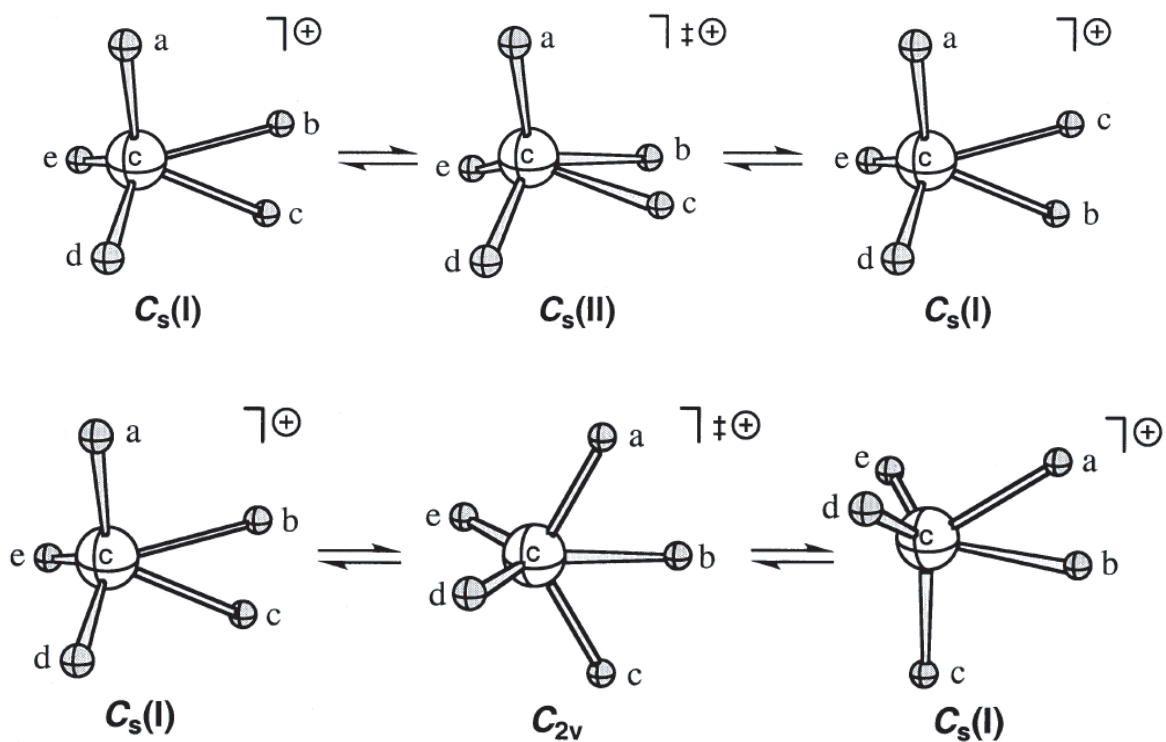


**Figure 2.1: Structures and interconversions of  $\text{CH}_5^+$**

The  $C_s(\text{I})$  structure is the Born-Oppenheimer potential minimum. Taking a semiclassical view of hydrogen scrambling, exchange of protons in the  $\text{H}_2$  unit occurs through the  $C_s(\text{II})$  transition state, and exchange of protons between the  $\text{CH}_3^+$  and  $\text{H}_2$  units occurs through the  $C_{2v}$  transition state. (Reprinted from Ref. 6.)

**Table 2.1: Evolution of stationary point energy differences in CH<sub>5</sub><sup>+</sup>**

Reference	Model Chemistry	$\Delta E$ (kcal/mol)	
		$C_s(\text{II})$	$C_{2v}$
Dyczmons <sup>8</sup>	SCF		5.6
Raghavachari <sup>17</sup>	SCF/6-31G*	0.04	3.82
	MP2/6-31G*	0.075	0.14
	SCF/6-31G**	0.04	3.43
	MP2/6-31G**	0.088	-0.49
von Ragué Schleyer <sup>19</sup>	QCISD(T)/6-311++G(3df,3pd)	-0.1	0.02
Schreiner <sup>3</sup>	CCSD(T)/TZ2P(f,d)	0.09	0.9
	CCSD(T)/TZ2P(f,d) with ZPVE corrections	-0.01	0.2
Müller <sup>4</sup>	BP86/cc-pV(5C,4H)Z	0.095	-0.388
	CCSD(T)R12/cc-pV(5C,4H)Z	0.097	0.818
Brown <sup>9</sup>	MP2/cc-pVTZ	-0.0303	-0.4306

All energies are referenced to the  $C_s(\text{I})$  structure. Negative energies represent states lower in energy than the  $C_s(\text{I})$  structure.

### 2.3 Classical and Quantum Dynamics of CH<sub>5</sub><sup>+</sup>

Given that stationary-point calculations indicate significant nuclear delocalization (or, semiclassically, internal motions), it is logical to attempt dynamics calculations to model the internal motions of CH<sub>5</sub><sup>+</sup>. Molecular dynamics treats nuclei classically, moving in a potential field which is usually determined quantum-mechanically. Propagation is accomplished simply by integrating the Newtonian equations of motion. The position  $\vec{Q}_k$  of the  $k$ th nucleus after a timestep of  $\Delta t$  is

$$\vec{Q}_k(t + \Delta t) = \vec{Q}(t) + \Delta t \left( \frac{d\vec{Q}_k}{dt} \right) - (\Delta t)^2 \frac{1}{2M_k} \nabla V(\vec{Q}(t)) \quad (2.5)$$

where  $M_k$  is the mass of the nucleus and  $V$  is the potential at that configuration, determined in any number of ways. One may determine  $V$  (rather inefficiently) by running electronic structure calculations on a grid of all molecular degrees of freedom. *Ab initio* molecular dynamics (AIMD) generates the potential “on the fly” by performing an electronic structure calculation at each classical timestep. Car-Parrinello molecular dynamics

(CPMD) is a specific case of AIMD, developed some time ago and employing density functional theory (DFT) as the electronic structure method.<sup>20</sup>

Quantum dynamics calculations, on the other hand, treat the nuclei fully quantum-mechanically, propagating the total nuclear wavefunction on a predetermined potential surface. Quantum dynamics calculations typically use either path integral techniques to propagate the wavefunction directly or Monte Carlo simulation of the motion of wavepackets on the potential surface. Both have been applied to  $\text{CH}_5^+$ .<sup>9,21</sup>

Most recently, diffusion Monte Carlo (DMC) quantum dynamics calculations have been used to generate the (vibrational) ground-state wavefunction on an *ab initio* potential surface.<sup>9,22,23</sup> Such calculations exploit the mathematical similarity of the Schrödinger equation (Eq. 2.6) to the classical diffusion equation (Eq. 2.7) with a first-order probability of reaction  $k$ :

$$-i\hbar \frac{\partial \Psi}{\partial t} = \frac{\hbar^2}{2m} \nabla^2 \Psi - V \Psi \quad (2.6)$$

↓

$$\frac{\partial C}{\partial t} = \mathcal{D} \nabla^2 C - kC \quad (2.7)$$

By performing a transformation to so-called imaginary time ( $t \rightarrow \tau = it/\hbar$ ), the Schrödinger equation takes a form identical to the above diffusion equation. A random walk simulation of a diffusion process may then be used to calculate the ground-state wavefunction given knowledge of the potential surface  $V$ .<sup>24</sup>

### 2.3.1 Early Dynamics Efforts

The first dynamics effort applied to  $\text{CH}_5^+$  was the use of CPMD by Tse *et al.* in 1995. Within this simulation, the  $\text{CH}_3^+ - \text{H}_2$  structure was clearly seen, as was large-amplitude proton motion indicating scrambling. The vibrational density of states (related to the vibrational spectrum) was calculated from the Fourier transform of the atom velocity auto-

correlation function, and showed state density extending from near zero past 3000  $\text{cm}^{-1}$ . This further indicated significant internal motion.<sup>25</sup>

Shortly thereafter, Marx and Parrinello reported a CPMD simulation including nuclear quantum dispersion calculated with a path integral methodology, thus including nuclear delocalization in a fully quantum-mechanical framework. Bond distance distributions were significantly broadened upon inclusion of quantum nuclear dispersion, giving direct evidence of proton tunneling. The bimodal bond length distribution indicated, however, that the  $\text{CH}_3^+ - \text{H}_2$  partitioning of  $\text{CH}_5^+$  may remain even in the presence of internal motion and proton tunneling. As the authors state succinctly, “ $\text{CH}_5^+$  undergoes large-amplitude pseudorotations, which result in hydrogen scrambling and statistically-equivalent protons. Nevertheless, there is an overwhelming probability of finding  $\text{CH}_5^+$  in a structure similar to the classical [ $C_s(\text{I})$  global minimum].”<sup>21</sup>

### 2.3.2 Recent Dynamics Efforts

The first dynamics simulations considered only nuclear motion, but more recently, diffusion Monte Carlo simulations have been used to calculate the ground-state nuclear wavefunction probability density directly. As in the prior CPMD simulations, the potential surface was generated with *ab initio* molecular dynamics. However, upon evidence that density functional theory produces different state orderings for the low-lying stationary points of  $\text{CH}_5^+$ ,<sup>4</sup> the explicitly-correlated MP2 method was used to generate the potential. DMC simulations were run on the resulting surface, with attention to enforcing proton permutation symmetry. These simulations showed statistical equivalence of the 120 minima, indicating widespread hydrogen exchange. However, they also showed bimodal character in the hydrogen-hydrogen distance distribution, indicating a preference for the  $\text{CH}_3^+ - \text{H}_2$  partitioning. An examination of probability projections onto coordinates corresponding to transitions across the  $C_s(\text{II})$  and  $C_{2v}$  transition states showed clearly an-

harmonic and delocalized behavior. In fact, it appears that  $\text{CH}_5^+$  is more likely to be found crossing through these two low-lying transition states than at the global  $C_s(\text{I})$  minimum.<sup>9</sup>

In addition to the DMC simulations, a classical dynamics simulation was run on the same potential surface. At energies well below the calculated zero-point vibrational energy, the classical system sampled all 120 minima, indicating highly-anharmonic behavior. Results of the classical MD simulation generally mirrored those taken from the DMC simulation, with slight variance readily assigned to the inherent inability of the classical simulation to take quantum dispersion effects into account.<sup>9</sup> This indicates that while tunneling plays a role in the delocalization and rearrangement of the protons in  $\text{CH}_5^+$ , most of the important dynamics are well-modeled with classical analogies, such as the consideration of hydrogen exchange as internal motion.

## 2.4 The Particle-on-a-Sphere Model

Both the classical MD and quantum DMC simulations yield a unimodal (though slightly-skewed) C-H bond length distribution in  $\text{CH}_5^+$ .<sup>9,26</sup> This implies that the pseudorotational motion in  $\text{CH}_5^+$  may be well-described by consideration of five particles on a sphere (POS), in analogy to the famous introductory particle-in-a-box potential.<sup>27</sup>

In the limit of separability of radial stretching from proton rearrangement about the central carbon, this approach shows promise as it reduces the dimensionality of the problem from exponential in the number of particles to *linear* in the number of particles, thus making converged numerical calculations of internal motion energy levels possible. First results indicate that this POS model reproduces the rotational levels of  $\text{CH}_4$  and the inversion splitting of  $\text{NH}_3$  fairly well<sup>27</sup>. Such a model may be useful in the analysis of  $\text{CH}_5^+$  spectra, but the  $\sim 1.25\text{\AA}$  width of the C-H distance distribution obtained by Brown *et al.* shows that the protons of  $\text{CH}_5^+$  are not rigidly confined to a sphere, but instead distributed radially with a relatively wide Gaussian-type distribution.<sup>9</sup> The separation of angular co-

ordinates from radial coordinates of the five protons may therefore also be problematic, perhaps reducing the utility of the POS model.

## 2.5 Symmetry Analysis

If the barriers to hydrogen exchange are indeed as trivially low as calculations indicate, then all particle exchanges are feasible, and any permutation-inversion analysis must be carried out in the full 240-dimensional  $G_{240} \equiv S_5^* = S_5 \otimes E^*$  group. The total wavefunction will be restricted to  $A_2^+$  symmetry, which is antisymmetric with respect to odd permutations of protons and unchanged by inversion.

### 2.5.1 Nuclear Spin Statistics

Nuclear spin is invariant under spatial inversion, so analysis is carried out in the  $S_5$  permutation group. As is readily shown by application of the symmetry elements to all possible spin states,

$$\Gamma_{\text{spin}} = 6A_1 \oplus 4G_1 \oplus 2H_1 \quad (2.8)$$

Or, using the ‘‘Almighty Formula’’ for addition of angular momenta,

$$(\mathcal{D}_{1/2})^5 = \mathcal{D}_{5/2} \oplus 4\mathcal{D}_{3/2} \oplus 5\mathcal{D}_{1/2} \quad (2.9)$$

Both readily indicate 6:16:10 spin statistical weights.

### 2.5.2 Equivalent Rotations of $\text{CH}_5^+$

Within the permutation-inversion world-view, the coupling of rotational states to nuclear spin states is analyzed by computing the ‘‘equivalent rotations’’ of permutation-inversion operations.<sup>28</sup> Since rotational wavefunctions are readily described as functions of the Eu-

ler angles defining the molecular reference frame, an equivalence must be derived between the permutation-inversion symmetry operations and functions of the Euler angles. The symmetry groups of these functions may then be derived, and the coupling of rotational states to other components of the total wavefunction determined.

The Euler angles  $\theta$ ,  $\phi$ , and  $\chi$  define a linear (rotational) map between a space-fixed axis system and the molecule-fixed axis system which maximizes the separation of rotational and vibrational motion:

$$\vec{q}_{\text{molec}} = \mathbf{\Lambda}(\theta, \phi, \chi) \vec{q}_{\text{space}} \quad (2.10)$$

where  $\mathbf{\Lambda}$  is a matrix of direction cosines in the Euler angles, which are constant for a fixed structure. The Euler angles themselves may be calculated merely as a rotation between a space-fixed frame and the principal axes, or as the rotation between a space-fixed frame and the Eckart axes, which minimize Coriolis coupling. The nuclear coordinates  $\vec{q}_i$  in the Eckart frame satisfy

$$\vec{J}_{\text{vib}} = \sum_i m_i \vec{q}_{0(i)} \times \frac{d\vec{q}_i}{dt} \approx \vec{0} \quad (2.11)$$

where  $\vec{q}_{0(i)}$  is an equilibrium configuration for nucleus  $i$ , which satisfies  $\vec{q}_i - \vec{q}_{0(i)} \approx \vec{0}$ .<sup>28</sup>

This presents an immediate difficulty for fluxional species such as  $\text{CH}_5^+$ . Without an unambiguous reference structure with respect to which to perform the rotational and vibrational analysis, the Euler angles are ambiguously-defined, at best. The Eckart frame becomes mathematically meaningless, as it depends completely on the selection of a unique vibrational equilibrium configuration which does not vary on the rotational timescale. As vibrational motion ( $\sim 10^{12} - 10^{13}$  Hz) occurs on a faster timescale than rotational motion ( $\sim 10^9$  Hz), the presence of large-scale internal motion will likely disrupt the separation of vibrational and rotational motion. However, if the internal motion of the molecule occurs on a timescale sufficiently short relative to the rotational motion, so-called ‘‘vibrational averaging’’ may lead to separability of rotational motion at the expense of knowledge about the structure of the molecule, as discussed in Section 3.1.

# Chapter 3

## Predicted Spectral Features of $\text{CH}_5^+$

### 3.1 Rotational Features

The rotational structure of the  $\text{CH}_5^+$  spectrum is perhaps the most complex issue of all. As described above, the rigid rotor model implicitly assumes a well-defined, fixed structure, from which the moment of inertia tensor is calculated in a discrete manner as

$$\mathbf{I} = \sum_i m_i \begin{bmatrix} y_i^2 + z_i^2 & -x_i y_i & -x_i z_i \\ -x_i y_i & x_i^2 + z_i^2 & -y_i z_i \\ -x_i z_i & -y_i z_i & x_i^2 + y_i^2 \end{bmatrix} \quad (3.1)$$

where  $m_i$  is the mass of the  $i$ th nucleus. The principal moments of inertia  $I$  are then given by the eigenvalue problem  $\mathbf{I}\omega = I\omega$ . The axes which diagonalize the moment of inertia tensor are the principal axes, which are used in the familiar manner to define the rotational states of the molecule. A mapping of permutation-inversion operations to rotations about the principal axes gives the symmetry labels of the rotational wavefunctions.

This analysis is fundamentally dependent both on the fixed structure of a molecule and the separability of vibrational and rotational motion. Neither condition is likely to hold for  $\text{CH}_5^+$ . In this case, well-defined vibrational and rotational levels may break down. However, it may not be unreasonable to view the ion as undergoing “vibrational averaging,” in which the internal motion leads to a system of apparently higher symmetry and better-defined rotational levels. Alternatively, in the static picture, the delocalized wavefunction is of higher symmetry than those of localized Born-Oppenheimer structures.

Given knowledge of the delocalization of the nuclei, one can calculate expectation values of the principal moments of inertia, and thus calculate expectation values of the rotational “constants.” Since the position operators are well-defined, the moment of inertia tensor must also be a well-defined operator, as

$$\langle \mathbf{I} \rangle = \int \mathbf{I}(\vec{q}) |\Psi(\vec{q})|^2 d\vec{q} \quad (3.2)$$

The diagonalization of  $\mathbf{I}$  can be accomplished in two ways. First, the expectation value of  $\mathbf{I}$  may be calculated, and the resulting tensor diagonalized. This is equivalent to calculating the principal moments of the most probable delocalized system. Second, the expectation value of the principal moments of inertia may be calculated by diagonalizing the moment of inertia tensor at every stage of the expectation value calculation, giving instead the most probable principal moments of inertia.

Such calculations are readily performed given a working knowledge of the probability density as a function of nuclear configuration, such as that calculated by the Bowman and McCoy groups by diffusion Monte Carlo methods. Both methods have merits and difficulties. The post-diagonalization of the moment of inertia tensor requires specifying molecule-fixed axes, calculating the moment of inertia tensor in that coordinate system, and then diagonalizing. Such a specification is ambiguous, as in the absence of a definite structure no unique axis system should be preferred. Preliminary results from the McCoy group indicate that there is no statistical difference in the rotational constants calculated by fixing the axes to the principal axes of the  $C_s(\text{I})$ ,  $C_s(\text{II})$ , and  $C_{2v}$  structures,<sup>23</sup> partially ameliorating this concern. On a more fundamental level choosing a molecule-fixed axis implies separability of vibrational and rotational angular momentum, which may lead to rotational constants with artificially-small variances.

The diagonalization of the axis system for every configuration, followed by averaging, dispenses with the need for fixing an axis system, and does not presume complete separa-

**Table 3.1: Rotational constants of  $\text{CH}_3^+$  calculated as in Eq 3.3.**

	$\tilde{A}$	$\tilde{B}$	$\tilde{C}$
Moments of Inertia ( $/10^{-40} \text{ g} \cdot \text{cm}^2$ )	7.01	7.42	7.45
Rotational Constants ( $\text{cm}^{-1}$ )	4.0	3.8	3.8
St. Dev. in Rotational Constants ( $\text{cm}^{-1}$ )	0.6	0.4	0.4
McCoy Rotational Constants ( $\text{cm}^{-1}$ )	$3.91 \pm 0.03$	$3.86 \pm 0.03$	$3.84 \pm 0.02$

The data from the McCoy group, provided for reference, are calculated as in Eq. 3.4, and reported for space-fixed axes corresponding to the principal axes of the  $C_{2v}$  transition state.<sup>23</sup>

tion of vibrational and rotational motion. Since the configurations used in the calculation are generated by DMC, which effectively models internal motion, diagonalization of the moment of inertia tensor for each configuration should give an indication of the variance to be expected in the rotational constants as a result of vibration-rotation coupling.

Such instantaneous diagonalization was performed on the McCoy group’s DMC data. Each data point from the DMC simulation consisted of a nuclear configuration and number of DMC descendents, which gives a relative probability for that configuration. At each point, the moment of inertia tensor  $\mathbf{I}$  was calculated and diagonalized, yielding the three principal moments of inertia  $I_{A,B,C}$ . The average was then obtained by weighting each set of principal moments by the number of DMC descendents and normalizing to the total number of descendents. Thus for nuclear configurations  $Q$  and number of descendents  $N$ ,

$$\langle I_{A,B,C} \rangle = \frac{\sum_i I_{A,B,C}(Q_i) N_i}{\sum_i N_i} = \frac{\sum_i \text{eig}(\mathbf{I}(Q_i)) N_i}{\sum_i N_i} \quad (3.3)$$

where  $\text{eig}(\mathbf{I})$  represents the set of eigenvalues of the matrix  $\mathbf{I}$ . This is in contrast to the McCoy group’s calculation, where

$$\langle I_{A,B,C} \rangle = \text{eig}(\langle \mathbf{I} \rangle) = \text{eig} \left( \frac{\sum_i \mathbf{I}(Q_i) N_i}{\sum_i N_i} \right) \quad (3.4)$$

The resulting principal moments are summarized in Table 3.1. The McCoy group’s

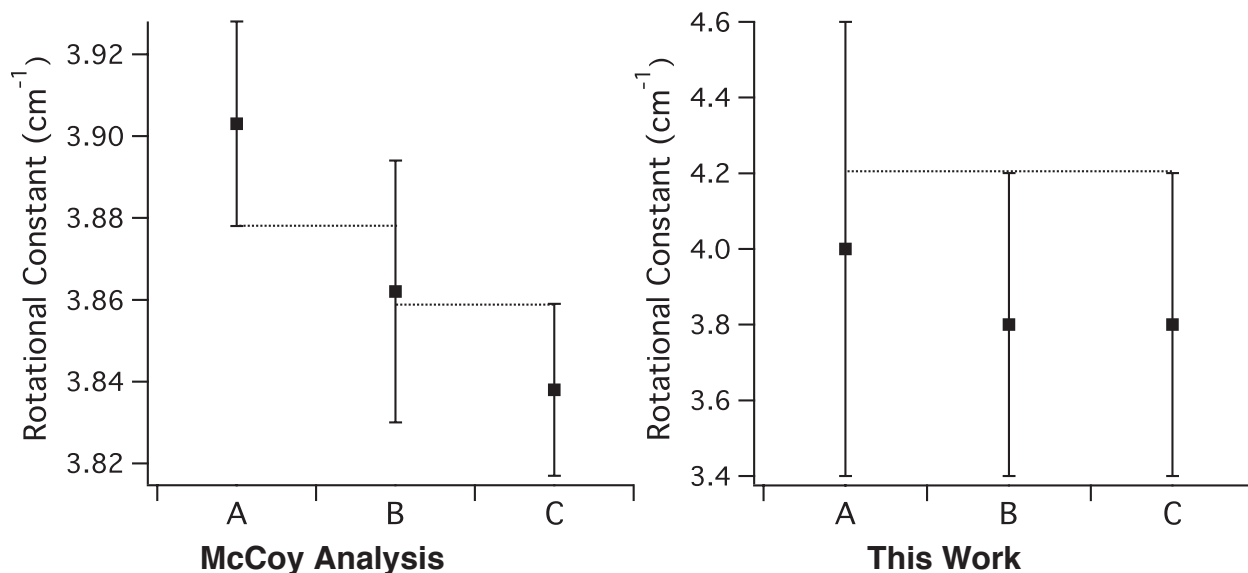


**Figure 3.1: Variation in rotational constants for post- (left) and instantaneous- (right) diagonalization.**

The dotted lines demarcate the possible rotational regimes: prolate or oblate symmetric top for the McCoy analysis, or any rotational symmetry for this work..

analysis unambiguously shows  $\text{CH}_5^+$  to be a symmetric top. However, the statistical uncertainties indicate that the molecule may be either prolate or oblate, as illustrated in Fig. 3.1. The prolate top is consistent with the  $\text{H}_2$  unit rotating freely with respect to the  $\text{CH}_3^+$  unit, giving a  $C_{3v}$  structure in which the  $\text{H}_2$  is delocalized into a toroid. The oblate top is consistent with free rotation delocalizing *both* subunits into toroids above and below the central carbon, and hydrogen exchange between the subunits merging the density into an oblate ellipsoid. Either case implies that the pure rotational spectrum of  $\text{CH}_5^+$  exists, and that a rotational spectrum of  $\text{CH}_5^+$  will be a direct indicator of the freedom of exchange pathways. A low barrier for exchange between the  $\text{CH}_3^+$  and  $\text{H}_2$  subunits will yield an oblate top spectral pattern, and a high barrier for exchange will yield a prolate top spectral pattern. The instantaneous-diagonalization scheme of Eq. 3.3, on the other hand, indicates that  $\text{CH}_5^+$  may take any rotational symmetry, from asymmetric top to spherical top. A spherical top is consistent with complete hydrogen exchange freedom, and the other cases have been described above.

The rotational constant calculations from DMC data therefore present a continuum of possibilities which may be realized by experiment. The absence of a pure rotational spectrum — or the presence of a spherical top rotational pattern in a rovibrational spectrum — would indicate complete delocalization of all five protons. An oblate symmetric top rotational pattern would indicate slightly hindered exchange of protons between the  $\text{CH}_3^+$  and  $\text{H}_2$  units of  $\text{CH}_5^+$ . A prolate symmetric top pattern would demonstrate strongly-hindered exchange between subunits, at least in the absence of a vibrational excitation sufficient to induce barrier-crossing.

The entire preceding discussion hinges on the assumption of vibrational averaging. In the absence of vibrational averaging, coupling between rotational and vibrational states will result in spectral splitting and ill-predictable rotational-scale patterns. There is likely not a vibrationally-averaged asymmetric top pattern. If  $\text{CH}_5^+$  were an asymmetric top, one would be able to choose a unique reference structure, but delocalization will likely result in inseparability of motions referenced to that structure and a concordantly complex spectrum. In such a case, the variances of the instantaneous moments of inertia reveal the coupling between rotational and vibrational motion. If  $\text{CH}_5^+$  indeed exhibited small amplitude vibration around a minimum (with the possible exclusion of vibrational averaging in one or more modes), then the spread of the instantaneous moments of inertia would be small and one would expect good separation of vibrational and rotational motion. This case appears unlikely for  $\text{CH}_5^+$  based on the  $> 10\%$  standard deviations obtained above.

## 3.2 Vibrational Features

With the apparent inseparability of motion in  $\text{CH}_5^+$ , one would expect the prediction and interpretation of vibrational features to present difficulty similar to that expected for the rotational problem. Beyond the issue of separating rotational and vibrational motions,

it appears unlikely that harmonic approximations of vibrations will be at all useful. The classical simulations of Bowman and McCoy show clearly-anharmonic behavior, with large-amplitude motions effecting proton scrambling. The diffusion Monte Carlo simulations by the same authors show significant proton delocalization and tunneling. Both classical and quantum simulations differ markedly from harmonic-motion predictions in probability distributions along several coordinates, especially the modes corresponding to transitions across the  $C_s(\text{II})$  and  $C_{2v}$  transition states.<sup>9</sup>

Despite the limited applicability of harmonic excitation energy calculations, such calculations are computationally relatively easy to perform, requiring only the diagonalization of an appropriately-scaled Hessian of the Born-Oppenheimer potential energy with respect to nuclear displacements.<sup>5</sup> Continued numerical differentiation of the potential with respect to nuclear displacement can be used to determine anharmonic corrections to the vibrational frequencies.<sup>29</sup> Such anharmonic frequency calculations still implicitly assume the absence of coupling among vibrational modes. As this is unlikely to be the case in a “floppy” molecule like  $\text{CH}_5^+$ , an alternative approach is to expand the vibrational Hamiltonian in a basis of harmonic oscillator wavefunctions, thereby explicitly including coupling effects. Such an approach is used in the MULTIMODE code due to Brown’s group<sup>30</sup>

Such harmonic, anharmonic, and MULTIMODE frequencies were calculated and are reported in Table 3.2 for each of the  $C_s(\text{I})$ ,  $C_s(\text{II})$ , and  $C_{2v}$  stationary points of  $\text{CH}_5^+$ . The harmonic calculations were performed at the MP2/cc-pVTZ level of theory, to match the potential energy surface calculations performed by Brown *et al.*<sup>9,31</sup>. The MULTIMODE calculations were performed on a more recent (and higher accuracy) CCSD(T)/aug-cc-pVTZ energy surface.<sup>22,32</sup> The difference between predicted harmonic and anharmonic frequencies of  $\text{CH}_5^+$  indicates the degree of anharmonicity of each mode, and the difference between the MULTIMODE frequencies and the harmonic/anharmonic frequencies indicates the extent of coupling of normal modes. Though these calculations are only as good as their

underlying methods and basis sets, it appears that  $\text{CH}_5^+$  is indeed a highly-anharmonic molecule which undergoes marked coupling among vibrational modes.

Using their MP2/cc-pVTZ potential energy surface, members of the Bowman group have used classical dynamics to assess the degree of anharmonicity and coupling among vibrational modes. For a number of modes,  $\text{CH}_5^+$  was distorted from its equilibrium position along a normal coordinate to a potential energy equal to the predicted (harmonic) excitation energy of that mode. Classical molecular dynamics was then carried out, and the atom velocity autocorrelation function was calculated and used to produce vibrational power spectra. Of the three modes analyzed and reported, all showed shifts with respect to the predicted harmonic frequencies. Two of the three modes (labeled Modes 1 and 3 in Table 3.2) showed redistribution of energy throughout the spectrum, indicating a high degree of coupling. One mode (Mode 5) did not appear to dissipate its energy to other modes, though a red shift of  $122\text{ cm}^{-1}$  was observed. The power spectra for Modes 1 and 5 are shown in Fig. 3.2.

The anharmonic frequency calculation of this work predicts a red shift of  $101\text{ cm}^{-1}$  for the seemingly-uncoupled Mode 3, and the MULTIMODE calculations of the Bowman group predict a red shift of  $149\text{ cm}^{-1}$ . The apparent lack of coupling to other normal modes makes this mode an interesting target for high-resolution spectroscopy. It should be noted that the classical simulation was restricted to zero total angular momentum, and the quantum mechanical calculations do not account for rotation. Given the seeming inseparability of vibrational and rotational motion indicated in  $\text{CH}_5^+$ , the rovibrational spectrum of Mode 5 may not be any simpler than those of the other modes.

**Table 3.2: Harmonic, anharmonic, and MULTIMODE frequencies of CH<sub>5</sub><sup>+</sup>**

<i>C<sub>s</sub>(I)</i>				<i>C<sub>s</sub>(II)</i>			
Mode	$\nu_{\text{harm}}$	$\nu_{\text{anharm}}$	$\nu_{\text{MM}}$	Mode	$\nu_{\text{harm}}$	$\nu_{\text{anharm}}$	$\nu_{\text{MM}}$
1	3272	3081	3080.9	1	3279	3128	3072.2
2	3170	3042	3002.5	2	3134	3010	2953.2
3	3035	2858	2743.1	3	3077	2943	2884.5
4	2719	2658	2641.1	4	2749	2879	2649.9
5	2524	2423	2375.2	5	2502	2423	2347.8
6	1579	1748	1402.7	6	1612	1365	1476
7	1499	1449	1468.9	7	1502	1437	1445.5
8	1474	1332	1393.8	8	1479	1427	1429.9
9	1301	1208	1135.1/1309.0	9	1337	1269	1276.4
10	1288	1121	1118.3	10	1145	1313	1193.7
11	747	551	273.2	11	945	704	610.5
12	233	42	282.9	12	222i	550i	182.1
ZPVE	11420	11096	11019.8	ZPVE	11264	10897	11080.7

<i>C<sub>2v</sub></i>			
Mode	$\nu_{\text{harm}}$	$\nu_{\text{anharm}}$	$\nu_{\text{MM}}$
1	3286	3129	3067.8
2	3169	3026	2982.9
3	2904	2829	2887.8
4	2743	1653	2585.9
5	2676	2554	2391.9
6	1477	1447	1458.5
7	1456	1400	1395.1
8	1412	1426	1426.5
9	1321	1257	1293.4
10	1261	1193	1115.7
11	585i	943i	293.6
12	482	360	174.8
ZPVE	10801	10514	10987

All frequencies are in cm<sup>-1</sup>. Harmonic ( $\nu_{\text{harm}}$ ) and anharmonic ( $\nu_{\text{anharm}}$ ) vibrational calculations were performed with Gaussian 03<sup>33</sup> at the MP2/cc-pVTZ level of theory. MULTIMODE<sup>30</sup> calculations ( $\nu_{\text{MM}}$ ) were performed by the Bowman group and included four-mode coupling for the *C<sub>s</sub>(II)* and *C<sub>2v</sub>* geometries and five-mode coupling for the *C<sub>s</sub>(I)* geometry.<sup>32</sup> In the MULTIMODE calculation, mode 9 of the *C<sub>s</sub>(I)* geometry was resonance-split; both frequencies are reported.

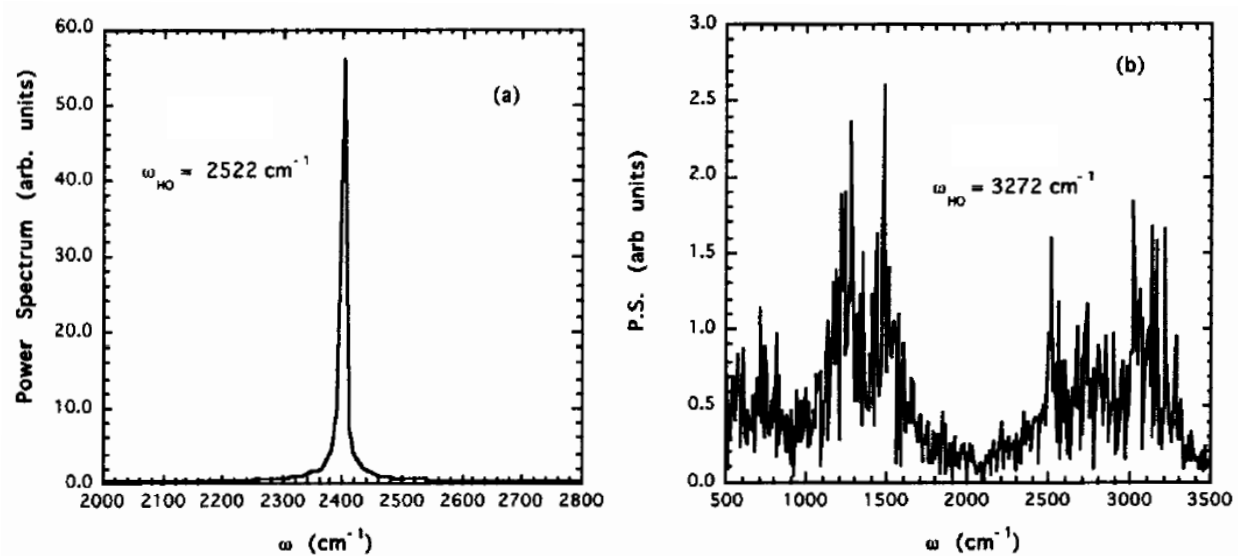


**Figure 3.2: Classical power spectra of CH<sub>5</sub><sup>+</sup> normal modes**

Panel (a) shows no coupling of Mode 5 (as labeled in Table 3.2) to other modes. Panel (b) shows the highly-coupled nature of Mode 1, with energy introduced only to this normal mode being redistributed throughout the molecule.<sup>31</sup>

# Chapter 4

## Summary, Conclusions, and Future Directions

The highly-fluxional nature of  $\text{CH}_5^+$  presents a number of challenges to traditional spectral prediction and interpretation. Spectral predictions to rotational accuracy currently appear out of reach. However, theoretical work has allowed for several qualitative and semi-quantitative predictions.

Stationary-point quantum chemical calculations are inherently limited by the Born-Oppenheimer approximation, which imposes a semi-classical picture on the structure and dynamics of  $\text{CH}_5^+$ . Though the BO approximation, mathematically, only separates nuclear and electronic motion, the resulting picture of point-mass nuclei moving on a potential surface is inherently classical. Quantum effects such as delocalization are most readily mapped to internal motion. Though such internal motion may indeed be the “reality” of the internal dynamics of  $\text{CH}_5^+$ , nuclear delocalization and tunneling may be an equally- (or more-) reasonable way to interpret the nature of  $\text{CH}_5^+$ . Widespread delocalization, as appears to be the case in  $\text{CH}_5^+$ , is ill-modeled by the classical concepts of structure and vibration.

Such widespread delocalization is implied by the low interconversion barriers between Born-Oppenheimer minima in multiple high-level stationary-point calculations. The diffusion Monte Carlo calculations of the Bowman and McCoy groups show dispersion of the wavefunction density from the starting point of the simulation into all 120 equivalent minima required by the exchange symmetry of the five protons, further supporting the highly-delocalized nature of  $\text{CH}_5^+$ .

Because of the absence of a unique equilibrium structure of  $\text{CH}_5^+$ , the separation of

rotational motion in the  $\text{CH}_5^+$  problem appears impossible except in the case of vibrational averaging. In that case, however, the observed rotational patterns will reveal much about the nature of  $\text{CH}_5^+$ . If the ion is a(n)

**spherical top**, then complete hydrogen delocalization imposes an apparent spherical symmetry in an inherently asymmetric problem.

**oblate symmetric top**, then the  $\text{CH}_3^+$  and  $\text{H}_2$  subunits of  $\text{CH}_5^+$  are chemically inequivalent, but relatively free hydrogen exchange occurs between the subunits.

**prolate symmetric top**, then the hydrogen nuclei are delocalized within each subunit, but hydrogen exchange does not occur particularly freely between units.

The very notion of molecular rotation is problematic for  $\text{CH}_5^+$ , since the ion is not well-described by small-amplitude vibrations around an equilibrium structure, as is evident from the large variances in the rotational constants obtained in the calculations of Section 3.1. The highly-anharmonic and -coupled nature of the vibrations of  $\text{CH}_5^+$ , as discussed in Section 3.2, further indicate that separation of motions in  $\text{CH}_5^+$  may be all but impossible in any rigorous manner. Given the apparent inseparability of vibrational and rotational motion, the only recourse for accurate calculation of the energy levels of  $\text{CH}_5^+$  (and subsequent ability to assign a spectrum) appears to be highly-accurate variational calculations.

## 4.1 Variational Calculations on $\text{CH}_5^+$

Variational calculations are the theoretical “gold standard” for comparison to spectroscopic experiments, because their accuracy is limited only by the number of variational parameters used, and therefore only by computational resources (time and memory) available. However, the exponential scaling of the variational problem with respect to system size rapidly reduces the practicality of such calculations.<sup>34</sup>

For instance, assume that some molecule’s ground-state wavefunction is well-desc-

ribed by some combination of  $N$  basis functions in each degree of freedom. For  $D$  degrees of freedom, then, there are  $N^D$  expansion coefficients in the resulting wavefunction. Assuming that it is reasonable to make the Born-Oppenheimer approximation and to calculate a sufficiently accurate nuclear potential energy surface, we may restrict our attention to the nuclear problem only, thus giving results to the rovibrational problem to within the accuracy of the potential energy surface. In such an approach, where  $N$  is typically  $\mathcal{O}(10)$ . A full rovibrational calculation on a  $n$ -center molecule contains  $3(n-1)$  degrees of freedom, so a three-center calculation would require optimization of  $10^6$  variables, a four-center calculation would require optimization of  $10^9$  variables and a six-center problem such as  $\text{CH}_5^+$  would require optimization of  $10^{15}$  variables.

One recent study by Yu<sup>34</sup> reduces the six-center vibrational problem to a seven-dimensional eigenvalue problem, reduces the optimization problem to superlinear complexity in the number of basis functions, and reduces the number of basis functions itself to  $\sim 10^9$ . The calculation still required approximately 225 CPU days to complete. Even if such a reduction could be used in the rovibrational problem, the addition of  $10^3$  variables with the three additional degrees of freedom would increase the running time of an  $\mathcal{O}(n^{1.5})$  calculation 30,000-fold. A Yu-style calculation for the rovibrational states of  $\text{CH}_5^+$  would then take approximately 18,000 CPU years. If only three basis functions were required to describe each degree of rotational freedom, the calculation would take fifteen CPU years. Even if the algorithm was easily parallelized — which it is not<sup>34</sup> — such a calculation far exceeds current computing capacity. Thus, it appears full-dimensional six-center rovibrational variational calculations remain out of reach with current computational technology and methodology.

## 4.2 Future Prospects

Though a high-resolution spectrum has recently been obtained by Nesbitt's group,<sup>35</sup> a cold spectrum free of interference from other species has yet to be reported. The results of vibrational MULTIMODE calculations have been applied to the low-resolution spectrum of Asvany *et al.*, yielding tentative vibrational assignments<sup>35</sup>. However, in light of the likely coupling between vibrational and rotational motion, the assignment of any levels may be premature. In the best case, careful examination of a cold, rotationally-resolved spectrum will reveal enough about the dynamics of  $\text{CH}_5^+$  to construct a reasonable model Hamiltonian. In the worst case, Oka's group may be proven correct in their assertion<sup>10</sup> that the only good quantum numbers (out of the familiar set) may be the total angular momentum, parity, and total nuclear spin angular momentum. In either case, the combination of spectroscopy, theory, and computation will reveal much about the nature of this enigmatic species, and how to think, in general, about systems which can neither be adequately described in semiclassical terms nor feasibly rigorously analyzed with the mathematics of quantum mechanics.

# References

- [1] Tal'roze, V. L.; Lyubimova, A. K. *Dokl. Akad. Nauk SSSR* **1952**, *86*, 909.
- [2] White, E. T. *High Resolution Infrared Laser Spectroscopy of CH<sub>5</sub><sup>+</sup>* PhD thesis, University of Chicago, **1999**.
- [3] Schreiner, P. R.; Kim, S.-J.; Schaefer III, H. F.; von Rague Schleyer, P. J. *Chem. Phys.* **1993**, *99*, 3716 – 3720.
- [4] Müller, H.; Kutzelnigg, W.; Noga, J.; Klopper, W. *J. Chem. Phys.* **1997**, *106*, 1863 – 1869.
- [5] Leach, A. R. *Molecular Modelling: Principles and Applications*; Pearson, 2nd ed., 2001.
- [6] Schreiner, P. R. *Angew. Chem. Int. Ed.* **2000**, *39*, 3239 – 3241.
- [7] Lathan, W. A.; Hehre, W. J.; Pople, J. A. *J. Am. Chem. Soc.* **1971**, *93*, 808 – 815.
- [8] Dyczmons, V.; Kutzelnigg, W. *Theo. Chim. Acta* **1974**, *33*, 239 – 247.
- [9] Brown, A.; McCoy, A. B.; Braams, B. J.; Jin, Z.; Bowman, J. M. *J. Chem. Phys.* **2004**, *121*, 4105 – 4116.
- [10] White, E. T.; Tang, J.; Oka, T. *Science* **1999**, *284*, 135 – 137.
- [11] Asvany, O.; Kumar, P.; Redlich, B.; Hegemann, I.; Schlemmer, S.; Marx, D. *Science* **2005**, *309*, 1219 – 1222.
- [12] Cafiero, M.; Bubin, S.; Adamowicz, L. *Phys. Chem. Chem. Phys.* **2003**, *5*, 1491 – 1501.
- [13] Dyczmons, V.; Staemmler, V.; Kutzelnigg, W. *Chem. Phys. Lett.* **1970**, *5*, 361 – 366.
- [14] Gamba, A.; Morosi, G.; Simonetta, M. *Chem. Phys. Lett* **1969**, *3*, 20 – 21.
- [15] Hariharan, P. C.; Lathan, W. A.; Pople, J. A. *Chem. Phys. Lett* **1972**, *14*, 385 – 388.
- [16] Sefcik, M. D.; Henis, J. M. S.; Gaspar, P. P. *J. Chem. Phys.* **1974**, *61*, 4321 – 4328.
- [17] Raghavachari, K.; Whiteside, R. A.; Pople, J. A.; v. R. Schleyer, P. J. *Am. Chem. Soc.* **1981**, *103*, 5649 – 5657.
- [18] Komornicki, A.; Dixon, D. A. *J. Chem. Phys.* **1987**, *86*, 5625 – 5634.

- [19] von Ragué Schleyer, P.; Walkimar, J. d. M. C. *J. Comp. Chem.* **1992**, *13*, 997 – 1003.
- [20] Car, R.; Parrinello, M. *Phys. Rev. Lett.* **1985**, *55*, 2471 – 2474.
- [21] Marx, D.; Parrinello, M. *Nature* **1995**, *375*, 216 – 218.
- [22] Jin, Z.; Braams, B. J.; Bowman, J. M. *J. Phys. Chem. A* **2006**, *110*, 1569 – 1574.
- [23] Johnson, L. M.; McCoy, A. B. *In press* **2006**.
- [24] Anderson, J. B. *J. Chem. Phys.* **1975**, *63*, 1499 – 1503.
- [25] Tse, J. S.; Klug, D. D.; Laasonen, K. *Phys. Rev. Lett.* **1995**, *74*, 876 – 879.
- [26] Thompson, K. C.; Crittenden, D. L.; Jordan, M. J. T. *J. Am. Chem. Soc.* **2005**, *127*, 4954 – 4958.
- [27] Deskevich, M. P.; Nesbitt, D. J. *J. Chem. Phys.* **2005**, *123*, 084304.
- [28] Bunker, P. R.; Jensen, P. *Molecular Symmetry and Spectroscopy*; NRC Research Press, 1998.
- [29] Clabo Jr., D. A.; Allen, W. D.; Remington, R. B.; Yamaguchi, Y.; Schaefer III, H. F. *Chem. Phys.* **1988**, *123*, 187 – 239.
- [30] Carter, S.; Culik, S. J.; Bowman, J. M. *J. Chem. Phys.* **1997**, *107*, 10458 – 10469.
- [31] Brown, A.; Braams, B. J.; Christoffel, K.; Jin, Z.; Bowman, J. M. *J. Chem. Phys.* **2003**, *119*, 8790 – 8793.
- [32] Huang, X. Personal communication.
- [33] Gaussian 03, revision b.04. Frisch, M. J.; others.; Gaussian, Inc., Pittsburgh, PA, **2003**.
- [34] Yu, H.-G. *J. Chem. Phys.* **2004**, *120*, 2270 – 2284.
- [35] Huang, X.; McCoy, A. B.; Bowman, J. M.; Johnson, L. M.; Savage, C.; Dong, F.; Nesbitt, D. J. *Science* **2006**, *311*, 60 – 63.